Matemática Contemporânea, Vol. 3, 191–209
http://doi.org/10.21711/231766361992/rmc312

SCATTERING BEHAVIOR OF TRANSITIONAL SHOCK WAVES

Kevin R. Zumbrun **Bradley J. Plohr**
Dan Marchesin

Abstract

We study the stability and asymptotic behavior of transitional shock waves as solutions of a parabolic system of conservation laws. In contrast to classical shock waves, transitional shock waves are sensitive to the precise form of the parabolic term, not only in their internal structure but also in terms of the end states that they connect. In our numerical investigation, these waves exhibit robust stability. Moreover, their response to perturbation differs from that of classical waves; in particular, the asymptotic state of a perturbed transitional wave depends on the location of the perturbation relative to the shock wave. We develop a linear scattering model that predicts behavior agreeing quantitatively with our numerical results.

1. Introduction

In this paper, we study the stability and behavior of transitional shock wave solutions of a system of two conservation laws with a quadratic flux and a viscous term with constant coefficients. Transitional waves arise in the study

1980 *Mathematics Subject Classification (1985 Revision).* 35B35, 35B40, 35L65, 35L67, 35L80.

Key words and phrases. conservation laws, non–strictly-hyperbolic, transitional shock waves, stability, scattering.

This work was supported in part by: the International Division of the National Science Foundation under Grant INT-9104216; the National Science Foundation Postdoctoral Program under Grant DMS-9107990; the National Science Foundation under Grant DMS 8901884; the U. S. Department of Energy under Grant DE-FG02-90ER25084; the U. S. Army Research Office under Grant DAAL03-91-C-0027 to the Mathematical Sciences Institute of Cornell University, through subcontract to Stony Brook; and the Conselho Nacional de Desenvolvimento Científico e Tecnológico (CNPq)

of Riemann problems for non-strictly-hyperbolic systems, for example in the equations of multiphase flow in porous media. They comprise a new family of traveling wave solutions, which are nonclassical in the sense that they do not satisfy the Lax characteristic criterion. As a consequence, the set of transitional wave solutions obtained in the zero-viscosity limit depends sensitively on the form of the viscosity matrix and not only on the hyperbolic structure of the equations.

Our motivation in this paper is twofold: first, the need to assess whether transitional waves represent physically meaningful solutions; second, the expectation that these waves should exhibit unusual and interesting behavior in their interaction with a perturbation. We address these issues by solving the Cauchy problem for the parabolic system using a finite difference scheme. As initial data, we take a perturbation of a single strong transitional wave.

In the models considered, we observe that transitional waves exhibit robust stability, emerging intact from interaction with even a strong perturbation. Furthermore, the interaction of the perturbing waves with the shock wave can be described simply as scattering phenomena. We develop a linearized scattering model that predicts the resulting shock shift and asymptotic distribution of mass. These predictions agree quantitatively with our numerical results, even for perturbations with rather large amplitude.

2. Transitional Shock Waves

We consider a system of two conservation laws,

$$U_t + F(U)_x = D\,U_{xx}, \tag{2.1}$$

where $F(U)$ is quadratic in U and D is a constant matrix with positive eigenvalues. We focus on models such that the corresponding hyperbolic system

$$U_t + F(U)_x = 0, \tag{2.2}$$

is strictly hyperbolic except at an isolated umbilic point $U = 0$ [8]. Thus the Jacobian $F'(U)$ has real eigenvalues $\lambda_i(U)$, $i = 1, 2$, which are distinct if $U \neq 0$,

and $F'(0)$ is a multiple of the identity matrix.

A traveling wave is a solution of system (2.1) having the form $U(x,t) = \hat{U}(x - st)$. Here s is called the shock speed, and the wave is said to connect the end states $U_- = \lim_{\xi \to -\infty} \hat{U}(\xi)$ and $U_+ = \lim_{\xi \to \infty} \hat{U}(\xi)$. In order for U to satisfy Eq. (2.1), $\hat{U}$ must be an orbit for the dynamical system

$$\hat{U}' = D^{-1} \left[-s(\hat{U} - U_-) + F(\hat{U}) - F(U_-) \right]. \tag{2.3}$$

The end states U_- and U_+ are critical points for this dynamical system, which means that (U_-, U_+, s) satisfies the Rankine-Hugoniot condition

$$-s(U_+ - U_-) + F(U_+) - F(U_-) = 0. \tag{2.4}$$

Therefore (U_-, U_+, s) represents a shock wave solution of the hyperbolic system, Eq. (2.2).

Not all triples (U_-, U_+, s) that satisfy the Rankine-Hugoniot condition arise from traveling waves. Correspondingly, in the hyperbolic theory, shock wave admissibility criteria, such as the classical Lax characteristic criterion, are needed to restrict the class of solutions. The Lax criterion, which prescribes that all but one characteristic must approach the shock wave, can be related to the traveling wave dynamical system as follows. Near a critical point U_c, solutions of the dynamical system approximately satisfy the linearized system

$$U' = D^{-1} \left[-s\, I + F'(U_c) \right] (U - U_c). \tag{2.5}$$

If $D = I$, then the eigenvalues of system Eq. (2.5) are $\lambda^i(U_c) - s$, $i = 1, 2$. Thus the Lax condition requires that either U_- is a saddle point and U_+ is an attracting node, or U_- is a repelling node and U_+ is a saddle point. In other words, the Lax condition implies the stability of the connecting orbit under perturbations of the dynamical system. This stability is maintained if D is close to a multiple of the identity matrix.

A *transitional wave* is defined to be a traveling wave such that U_- and U_+ are distinct saddle points. The phase portrait of the corresponding dynamical system is therefore unstable, in contrast to the case of a Lax wave. This implies

an important difference between Lax and transitional shock waves: for a fixed state U_-, consider the Hugoniot curve of solutions (U_-, U_+, s) of the Rankine-Hugoniot condition; then points on the Hugoniot curve that correspond to traveling waves of Lax type form an open subset, whereas points corresponding to waves of transitional type are generically isolated.

In the generic case, such an isolated point depends continuously on U_-. In other words, the Rankine-Hugoniot condition and the condition that a connecting orbit should exist can be combined into a single constraint

$$U_+ = T(U_-). \tag{2.6}$$

The function T is called the *transitional map* and plays a fundamental role in the behavior of transitional waves. An associated function is the *speed map*

$$s = \Sigma(U_-) \tag{2.7}$$

giving the shock speed in terms of the left end state.

In the present paper, we have focused on transitional waves in systems of conservation laws with a quadratic flux. A broad class of transitional waves has been identified for these systems, namely those for which the connecting orbit in the dynamical system is a straight line segment [4]. The viscous profiles for these shock waves, and therefore the transitional and speed maps, can be calculated analytically, as we show below. For simplicity, therefore, our numerical experiments and scattering model concern straight-line transitional waves. Although these transitional waves are special, we believe that their behavior is typical of general transitional waves. We emphasize that there is no obstacle to applying our numerical method or to extending our scattering model to general transitional waves. This is an object for future work.

There are two conditions for the existence of a straight-line shock wave. First, (U_-, U_+, s) must satisfy the Rankine-Hugoniot condition, which for a quadratic flux is

$$F'(\overline{U})\,\Delta U = s\,\Delta U\ , \tag{2.8}$$

where $\overline{U} := \frac{1}{2}(U_- + U_+)$ and $\Delta U := U_+ - U_-$. Second, the line segment from U_- to U_+ must be invariant for the dynamical system. This amounts to the condition that there should exist a $\mu < 0$ such that

$$\frac{1}{2}F''(0)\,(\Delta U)^2 = \mu D\,\Delta U\ . \tag{2.9}$$

The viscous profile is then $\hat{U} = \overline{U} + \rho\Delta U$, where $\rho(\xi) = \frac{1}{2}\tanh(-\mu(\xi - x_0))$ and x_0 is the shock wave location.

To calculate the transitional map T, we write $\Delta U = R\,(\cos\varphi, \sin\varphi)^{\mathrm{T}}$. Thus Eq. (2.9) becomes a cubic equation in $\tan\varphi$ depending solely on the flux coefficients and D. The solutions φ are called the *viscosity angles*. For each fixed viscosity angle φ, Eq. (2.8) is a linear equation that determines (R, s), and thereby U_+, in terms of U_-. More precisely [4] , we can write Eq. (2.8) in the form

$$(\alpha(\varphi), \beta(\varphi))\,\overline{U} + \gamma(\varphi) = 0\ , \tag{2.10}$$

$$(\tilde{\alpha}(\varphi), \tilde{\beta}(\varphi))\,\overline{U} + \tilde{\gamma}(\varphi) = s\ . \tag{2.11}$$

It follows that if $\alpha(\varphi)\cos\varphi + \beta(\varphi)\sin\varphi \neq 0$, which is the generic case, then both the transitional map and the speed map are affine linear, with derivatives

$$T'(U_-) = I - \frac{2}{\alpha(\varphi)\cos\varphi + \beta(\varphi)\sin\varphi}\begin{pmatrix}\cos\varphi\\ \sin\varphi\end{pmatrix}(\alpha(\varphi), \beta(\varphi)) \tag{2.12}$$

and

$$\Sigma'(U_-) = (\tilde{\alpha}(\varphi), \tilde{\beta}(\varphi)) - \frac{\tilde{\alpha}(\varphi)\cos\varphi + \tilde{\beta}(\varphi)\sin\varphi}{\alpha(\varphi)\cos\varphi + \beta(\varphi)\sin\varphi}\,(\alpha(\varphi), \beta(\varphi))\ . \tag{2.13}$$

Remarks.

(1) Equation (2.10) restricts $\overline{U}$ to lie on a line (the *characteristic line* at angle φ), parameterized, say, by κ. Consequently, the class of transitional shock waves can be parameterized by κ and R. The traveling wave solutions corresponding to pairs (κ, R) that lie on a given ray through the origin are all essentially the same, being related by scaling x and D in Eq. (2.1).

(2) Although some straight line shock waves are Lax connections, there exists, in general, an open wedge of points U_- such that $(U_-, T(U_-), \Sigma(U_-))$ is a transitional shock wave [4]. That the boundary between Lax and transitional shock waves comprises two straight lines follows from the aforementioned scaling relationship.

(3) We emphasize that the viscosity angles, and thus the pairs of end states $(U_-, T(U_-))$ that are allowable for transitional shock waves, depends on the choice of the viscosity matrix D. This is markedly different from the classical case, in which the viscosity affects only the internal structure of a shock wave.

3. Stability

Although transitional waves can be constructed by solving the dynamical system (2.3), the stability of these waves as solutions of the parabolic system is unclear. Indeed, transitional waves might not occur in "typical" solutions of Eq. (2.1). This could be because of their special nature as traveling waves connecting pairs of saddle points: the set of transitional wave solutions has higher codimension than the set of Lax traveling waves. If transitional waves were unstable, they would be unsuitable as components in solutions of Riemann problems.

Before discussing the stability of transitional waves, it is worthwhile reviewing stability considerations for classical shock waves. The weakest type of stability is what we term *hyperbolic stability*. For a given traveling wave solution of the parabolic system (2.1), there is a shock wave solution of the associated hyperbolic system (2.3) with the same speed and end states. Hyperbolic stability requires that the Cauchy problem for the hyperbolic system be well-posed for initial data being smooth, compact support perturbations of this shock wave.

In the hyperbolic stability problem, the shock wave represents a moving boundary with associated constraints linking the shock speed and the states on either side. By the method of characteristics, the Cauchy problem is well-posed

if the shock constraints exactly determine the shock speed and the amplitudes of waves emerging along outgoing characteristics. For classical shock waves in a system of n conservation laws, the shock constraints are simply the n Rankine-Hugoniot conditions, and hyperbolic stability reduces to the Lax criterion, which requires precisely $n-1$ outgoing characteristics at the shock wave.

A stronger requirement is that the Cauchy problem for the parabolic system be well-posed for compact support perturbations of the traveling wave; this we term *parabolic stability*. For weak classical shock waves, Liu [5, 6] has shown that the Lax criterion also implies parabolic stability. In fact, he shows that the time-asymptotic state for this problem consists of a translation of the original traveling wave together with "dissipation" waves moving along the characteristics leaving the shock wave. The dissipation waves decay in L^∞ but carry finite mass in the corresponding characteristic field.

An important feature of classical waves, which is essential to Liu's analysis, is that the shock shift and the masses for the $n-1$ outgoing dissipation waves are determined from the total mass of the perturbation by the n equations of mass conservation. In other words, the asymptotic state is completely determined by the mass of the perturbation. This makes feasible the strategy that Liu follows to prove stability: in the simplest terms, one linearizes around the known asymptotic state and seeks mechanisms of stability that dominate the nonlinear behavior.

The case of transitional shock waves is different. Focusing on $n = 2$, the Lax criterion is not satisfied because there are two outgoing characteristics. Thus for the hyperbolic problem, the two Rankine-Hugoniot conditions are not sufficient to determine the shock speed and outgoing waves. Likewise, even if the solution of the parabolic equations tends to an asymptotic state of the type described by Liu, the two equations of mass conservation do not determine the shock shift and two outgoing masses. Stated another way: just as local conservation of mass, as embodied in the Rankine-Hugoniot condition, is inadequate to determine the instantaneous behavior of the shock wave, global conservation of mass is inadequate to determine the time-asymptotic state.

We can easily resolve the indeterminacy at the instantaneous level by replacing the n Rankine-Hugoniot conditions by the $n+1$ conditions given by the transitional map together with the speed map. This establishes hyperbolic stability. However, the indeterminacy at large time remains. Any condition that supplements conservation of mass would seem to depend on the dynamics of wave interaction, integrated over time. In particular, the analysis of Liu is not applicable to transitional waves.

Nonetheless, we believe that transitional waves are also stable in the parabolic sense, and further that the indeterminacy of the asymptotic state, rather than being only a technical obstacle to proving stability, reflects interesting new behavior for these waves. These conjectures are supported by our numerical results, to be described in Sec. 5, which demonstrate both the stability of transitional waves under perturbation and the sensitivity of the asymptotic states to the distribution, and not only to the mass, of the perturbation. In the next section, we interpret the response of transitional waves to perturbations as a scattering phenomenon, and predict the asymptotic state to first order in the perturbation amplitude.

4. Scattering Model

The qualitative response of a transitional wave to a perturbation can be predicted by a simplified version of the hyperbolic model of Sec. 3. We consider a transitional shock wave from U_- to U_+, in coordinates where the shock speed is zero. In our simplified model, we fix the shock wave at $x = 0$, and linearize about the constant states on either side. More precisely, we solve the equations

$$U_t + F'(U_-)U_x = 0 \qquad \text{for } x < 0\,, \tag{4.1}$$

$$U_t + F'(U_+)U_x = 0 \qquad \text{for } x > 0\,, \tag{4.2}$$

and at $x = 0$, we impose the boundary condition

$$U(0^+, t) = U_+ + T'(U_-)\left[U(0^-, t) - U_-\right] \tag{4.3}$$

obtained by linearizing the transitional map $U(0^+,t) = T(U(0^-,t))$.

Although the underlying discontinuity is held fixed at $x = 0$, we can define an effective shock location using the linearized speed map. Thus our model predicts the speed of the shock wave to be

$$s(t) = \Sigma'(U_-)\left[U(0^-,t) - U_-\right] \tag{4.4}$$

and the shock shift to be the time integral of $s(t)$. As we shall see below, the error incurred by neglecting the motion of the discontinuity is of second order in the amplitudes of the perturbation, so that it may be ignored in the linearized problem. Moreover, by making this approximation, we obtain a linear problem.

Notice that we have neglected the dissipation term in Eqs. (4.1) and (4.2). Were these terms to be included, the principal effect would be the decay of outgoing waves. However, the outgoing masses and shock shift would be unaffected. The effects of dissipation are included in our simplified model only through the transtional map, Eq. (4.3). The success of our model indicates that the key to the behavior of transitional waves is the transitional map.

The first step in solving the model is to express the amplitudes of outgoing waves in terms of incoming amplitudes. Let $r_i(U)$, $i = 1,2$, be right eigenvectors of $F'(U)$ corresponding the the eigenvalues $\lambda_i(U)$. On the left side of the discontinuity, the eigenvectors corresponding to the incoming and outgoing characteristic directions are $r^i_- := r_2(U_-)$ and $r^o_- := r_1(U_-)$; similarly, on the right side, we have $r^i_+ := r_1(U_+)$ and $r^o_+ := r_2(U_+)$. The states can be expressed in terms of the incoming and outgoing amplitudes:

$$U(0^-,t) = U_- + a^i_- r^i_- + a^o_- r^o_- \,, \tag{4.5}$$

$$U(0^+,t) = U_+ + a^i_+ r^i_+ + a^o_+ r^o_+ \,. \tag{4.6}$$

In these terms, Eq. (4.3) can be solved to express the outgoing amplitudes as

$$\begin{pmatrix} a^o_- \\ a^o_+ \end{pmatrix} = M \begin{pmatrix} a^i_- \\ a^i_+ \end{pmatrix} \,, \tag{4.7}$$

where

$$M = \left(-T'(U_-)r^o_-, r^o_+\right)^{-1}\left(T'(U_-)r^i_-, -r^i_+\right) \,. \tag{4.8}$$

The speed is given by

$$s = N \begin{pmatrix} a_-^i \\ a_+^i \end{pmatrix} , \tag{4.9}$$

with N being the row vector

$$N = \Sigma'(U_-) \left[r_-^o (M_{11}, M_{12}) + r_-^i (1,0) \right] . \tag{4.10}$$

In the second step we derive a scattering matrix that relates the incoming masses of the perturbations on the left and right sides to the outgoing masses. Notice that the outgoing masses in the perturbation remain outgoing and do not interact with the shock wave; without loss of generality, we can assume that the perturbation has only incoming mass. Let us first treat the case of a square pulse incoming from the left, with amplitude a_-^i and width ℓ. Referring to Fig. 4.1, the length of time during which the pulse interacts with the shock wave is $\ell/|\lambda_-^i|$, and the lengths of the outgoing pulses on the left and right are $\ell|\lambda_-^o/\lambda_-^i|$ and $\ell|\lambda_+^o/\lambda_-^i|$, respectively. The outgoing amplitudes are obtained from Eq. (4.7). Finally, the outgoing masses are given by

$$m_-^o = |\lambda_-^o/\lambda_-^i| \, M_{11} \, m_-^i , \tag{4.11}$$

$$m_+^o = |\lambda_+^o/\lambda_-^i| \, M_{21} \, m_-^i , \tag{4.12}$$

in terms of the incoming mass $m_-^i = \ell \, a_-^i$. Since the shock speed is zero except during the interaction, the shock shift is the speed $s = N_1 \, a_-^i$ times the interaction time, i.e., $(N_1/|\lambda_-^i|) m_-^i$. Similar considerations apply on the right side of the shock wave. Furthermore, the same formulae apply when the incoming pulses are not square; this follows from the linearity of the problem.

Thus we are led to a linear scattering relationship

$$\begin{pmatrix} m_-^o \\ m_+^o \end{pmatrix} = S \begin{pmatrix} m_-^i \\ m_+^i \end{pmatrix} , \tag{4.13}$$

where

$$S = \begin{pmatrix} |\lambda_-^o/\lambda_-^i| \, M_{11} & |\lambda_-^o/\lambda_+^i| \, M_{12} \\ |\lambda_+^o/\lambda_-^i| \, M_{21} & |\lambda_+^o/\lambda_+^i| \, M_{22} \end{pmatrix} . \tag{4.14}$$

The shock shift is given by

$$\Delta x = X \begin{pmatrix} m_-^i \\ m_+^i \end{pmatrix} , \tag{4.15}$$

where

$$X = \left(N_1/|\lambda_-^i|\,, N_2/|\lambda_+^i|\right)\ . \tag{4.16}$$

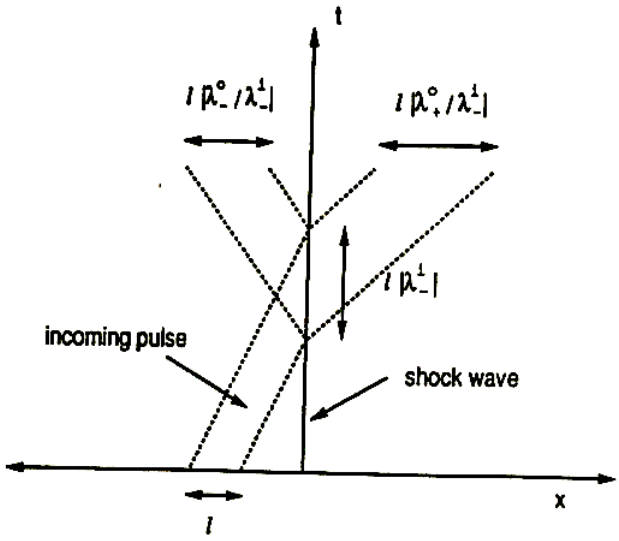

Figure 4.1. Characteristic portrait of a shock wave interacting with a perturbing pulse. In the linearized theory, a square pulse entering the transitional shock wave is converted to outgoing pulses on either side of the shock wave.

Remarks.

(1) Observe that neglecting shock movement amounts to approximating the true interaction time $\ell/(|\lambda_-^i| - N_1\, a_-^i)$ by $\ell/|\lambda_-^i|$. The difference between these times being $O(a_-^i)$, the error incurred by neglecting the motion of the discontinuity is of second order in the amplitudes of the perturbation, as claimed earlier.

(2) The reader can check that the total mass of the outgoing state predicted by the simple model is the same as the ingoing mass. This is a consequence of

the linearized Rankine-Hugoniot condition, which follows from Eqs. (4.3) and (4.4).

(3) For a Lax wave, the simplified model predicts the shock shift exactly. This follows from conservation of mass, since the characteristic speeds and eigenvectors of the end states are the same as for the parabolic model.

(4) We have implicitly assumed that M is defined, i.e., the vectors $T'(U_-)r_-^o$ and r_+^o are transverse. This is precisely the condition that the Riemann problem be well-posed for left and right states near U_- and U_+, respectively.

5. Numerical Experiments

To study the behavior of transitional waves we have implemented a finite-difference scheme to solve the parabolic system (2.1) numerically. In order to have second-order accuracy, we use a linearized Crank-Nicholson scheme, as implemented by Beam and Warming [1].

The scheme is specified more precisely as follows. Let the space and time grid spacings be Δx and Δt, respectively, and let $U_j^n := U(j\Delta x, n\Delta t)$ denote the solution values at the grid points. Then for each time step n, the increments $\delta U_j^n := U_j^{n+1} - U_j^n$ in time are obtained as the solution of the block-tridiagonal linear system

$$\frac{1}{\Delta t}\delta U_j^n + \frac{1}{2\Delta x}\left\{F(U_{j+1}^n) - F(U_{j-1}^n) + \frac{1}{2}F'(U_{j+1}^n)\,\delta U_{j+1}^n - \frac{1}{2}F'(U_{j-1}^n)\,\delta U_{j-1}^n\right\}$$
$$= \frac{1}{(\Delta x)^2}D\left\{U_{j+1}^n - 2U_j^n + U_{j-1}^n + \frac{1}{2}\left[\delta U_{j+1}^n - 2\delta U_j^n + \delta U_{j-1}^n\right]\right\} \qquad (5.1)$$

(In other words, we have made the approximation $F(U_j^{n+1}) \approx F(U_j^n) + F'(U_j^n)\,\delta U_j^n$ to avoid having to solve a nonlinear system of equations.)

The results from typical experiments are shown in Figs. 5.1–5.3. The model used in these experiments is

$$u_t + \left(\frac{1}{2}u^2 + 2uv - su\right)_x = \epsilon\left(u_{xx} + \frac{1}{2}v_{xx}\right)\,, \qquad (5.2)$$

$$v_t + \left(\frac{1}{4}u^2 - v^2 - sv\right)_x = \epsilon\left(\frac{1}{2}u_{xx} + v_{xx}\right) , \tag{5.3}$$

with $\epsilon = 1.5$ and $s = -0.197$.

For this model, there is a stationary transitional wave joining the states $U_- = (1, -0.1)^{\mathrm{T}}$ and $U_+ = (-1, -0.1)^{\mathrm{T}}$. (The linear terms in the fluxes of Eqs. (5.2) serve only to keep this transitional wave stationary.) The eigenvalues and eigenvectors are

$$\begin{aligned}
\lambda_-^o &= -0.35 , & r_-^o &= \begin{pmatrix} -0.83 \\ 0.56 \end{pmatrix} , \\
\lambda_-^i &= \ \ 1.74 , & r_-^i &= \begin{pmatrix} -0.94 \\ -0.35 \end{pmatrix} , \\
\lambda_+^i &= -1.52 , & r_+^i &= \begin{pmatrix} 0.97 \\ 0.25 \end{pmatrix} , \\
\lambda_+^o &= \ \ 0.91 , & r_+^o &= \begin{pmatrix} 0.72 \\ -0.69 \end{pmatrix} .
\end{aligned} \tag{5.4}$$

The scattering matrix for this transitional wave, which corresponds to viscosity angle $\varphi = 0$, is

$$S = \begin{pmatrix} -0.0823 & 0.201 \\ 0.440 & -0.206 \end{pmatrix} , \tag{5.5}$$

and the shift vector is

$$X = (-0.662, 0.642) . \tag{5.6}$$

The initial data for the experiments were perturbations of the Riemann problem with $U_L = U_-$ and $U_R = U_+$.

In the experiment of Fig. 5.1, the Riemann problem was perturbed by a square wave containing only an incoming wave on the right. (The state inside the perturbing pulse is $U = (-1.395, -0.199)^{\mathrm{T}}$.)

The four frames of Fig. 5.1 show the first component u of U plotted *vs* x. The initial data is shown in Fig. 5.1a, and Fig. 5.1b shows the solution at a typical time during the interaction of the perturbation with the shock wave. Figure 5.1c shows the solution at a late time, which we interpret as the time-asymptotic state. We see that the transitional shock wave has emerged intact, and that the asymptotic state consists of a shifted shock wave together with outgoing dissipation waves. In the final frame, Fig. 5.1d, we show the asymptotic

state in finer detail near the shock wave. In this picture, we have superimposed the viscous profile determined analytically and positioned as predicted by the scattering model: $\hat{U} = \overline{U} + \rho\Delta U$, where $\rho(\xi) = \frac{1}{2}\tanh(-\mu(\xi - \Delta x))$, μ is determined from Eq. (2.9), and Δx is given in Eq. (4.15).

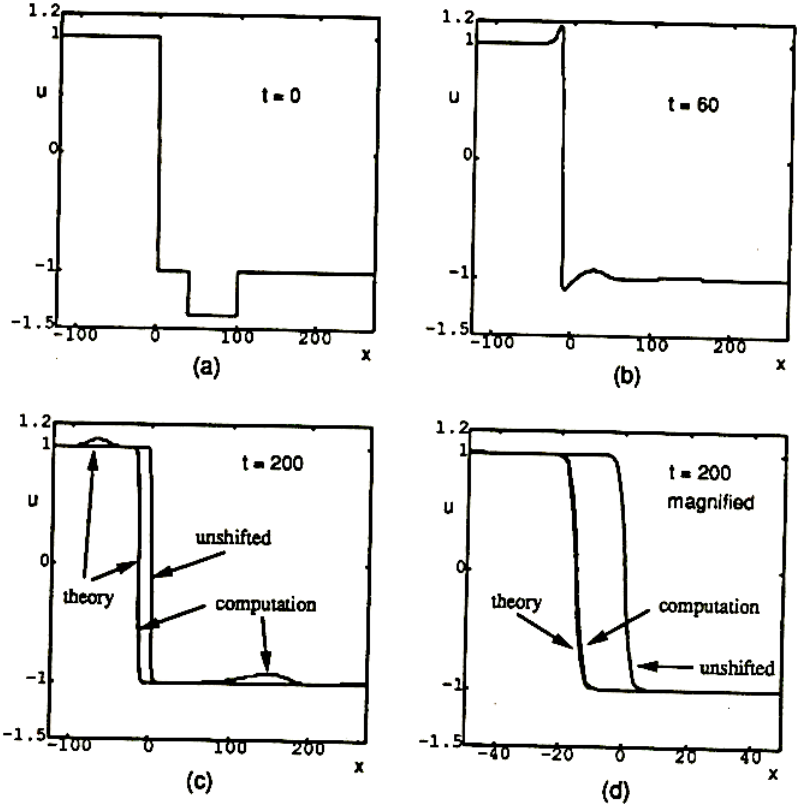

Figure 5.1. The results of the interaction of a transitional shock wave with a perturbation. Plots of u *vs* x are shown at different times: (a) the initial data; (b) during the interaction process; (c) after the interaction (with outgoing pulses shown); (d) after the interaction, on a magnified spatial scale. Superimposed on plots (c) and (d) are the profile at the initial position and the asymptotic profile predicted by the scattering model of Sec. 4.

We draw two conclusions from a visual comparison of the numerical and an-

alytic profiles. First, since the shape of the numerical profile so closely matches the analytic profile, any numerical viscosity in the scheme is small compared to D. Second, since the positions of the waves agree, the simple scattering model of Sec. 4 is accurate, even though the perturbing wave has a large amplitude.

In Fig. 5.2 is shown a contour plot of u as a function of both x and t, which shows how the transitional shock wave shifts as a result of interacting with the perturbation. Note the similarity between this figure and Fig. 4.1.

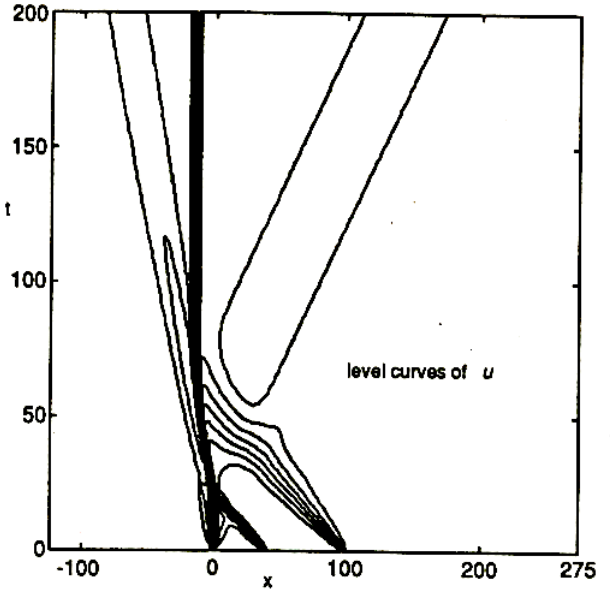

Figure 5.2. A contour plot of u in the (x,t)–plane for the interaction problem described in Fig. 5.1.

In the experiment of Fig. 5.3, the Riemann problem was perturbed by square waves on both the left and right sides, the total mass of the perturbation being zero. (The state inside the perturbing pulse on the left is $U = (1.1, -0.3)^{\mathrm{T}}$,

whereas on the right the perturbing state is $U = (-1.1, 0.1)^{\mathrm{T}}$.) The four frames of Fig. 5.3 are as in Fig. 5.1.

The final frame (d) of Fig. 5.3 shows that there is a nonzero shift resulting from the interaction of the transitional wave with the perturbation, despite that the total mass of the perturbation is zero.

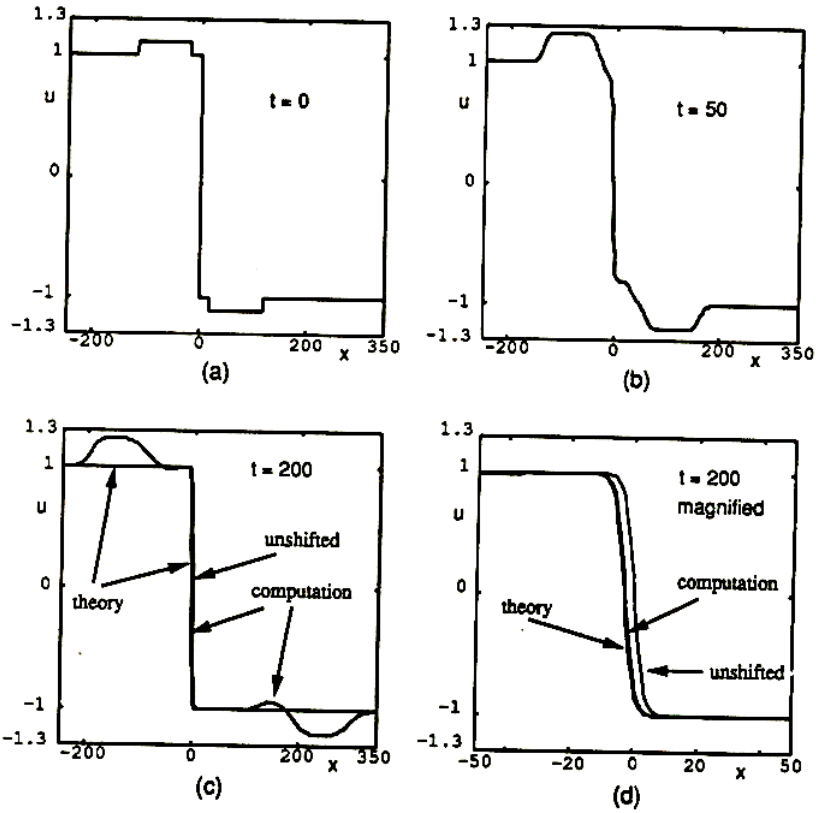

Figure 5.3. The results of the interaction of a transitional shock wave with a perturbation with zero total mass. Plots of u *vs* x are shown at different times: (a) the initial data; (b) during the interaction process; (c) after the interaction (with outgoing pulses shown); (d) after the interaction, on a magnified spatial scale. Superimposed on plots (c) and (d) are the profile at the initial position and the asymptotic profile predicted by the scattering model of Sec. 4.

By contrast, a Lax wave interacting with a perturbation with zero total mass would suffer no shift. Notice that the shift is rather small even though the perturbing masses are large. (The shift is -3.30 theoretically and -2.84 in the computational experiment, while the incoming masses are 13.6 on the left and 8.85 on the right.) This is because the two components of the shift vector X are nearly equal and opposite.

In fact, the shift is the result of balancing a shift of -8.98 caused by the left pulse and a shift of 5.68 caused by the right pulse. In this light, the discrepancy between the theoretical and computationally observed shock shift is less than 10%.

6. Conclusions

We may draw several conclusions from our numerical studies. At the least, the results appear to confirm the suitability of transitional waves as components of solutions of Riemann problems. Indeed, the large-time limit of a solution of a Riemann problem for a parabolic system is equivalent, by scaling, to the zero-dissipation limit: if $V(x,t) := U(x/\epsilon, t/\epsilon)$, then V satisfies Eq. (2.1) with D replaced by ϵD, as well as the same Riemann initial conditions as does U; the limit $\epsilon \to 0$ gives the large-time limit for U and the zero-dissipation limit for V. Thus the observed convergence to traveling waves at large time implies that transitional waves are vanishing-viscosity solutions of Riemann problems. (This result is much stronger than mere existence of a viscous profile, which is obtained as the limit of solutions whose initial data vary with viscosity.) Further, the stability of transitional waves under perturbation indicates that transitional waves should be persistent and recognizeable features in solutions to the parabolic equations.

More intriguing is the nonclassical response of transitional traveling waves to perturbation, which illustrates the richness of behavior possible in non-strictly-hyperbolic systems. We have demonstrated a close correspondence between the computed asymptotic behavior of a perturbed wave and the predictions of our

scattering model. One prediction is that the asymptotic state of a transitional shock wave is not determined by the perturbing mass alone, in contrast to the case of a classical shock wave [5]. Our scattering model quantifies the asymptotic state to first order by accounting for the masses on the two sides of the wave separately; this is accomplished by invoking the transitional map. Further details about the asymptotic state presumably depend on finer structure of the perturbation, in a complicated and essentially dynamic way.

We note that the concept of the Riemann problem as a scattering phenomenon has been advanced by Glimm in more general contexts (see, *e.g.*, Refs. [3, 2]).

Acknowledgments

One of the authors (DM) thanks his hosts at Stony Brook for their hospitality during his sabbatical leave. The other authors thank IMPA for a pleasant visit, during which this manuscript was prepared.

References

[1] R. Beam and R. Warming, *An Implicit Finite Difference Algorithm for Hyperbolic Systems in Conservation-Law Form*, J. Comput. Phys., 22 (1976), 87–110.

[2] J. Glimm, *Nonuniqueness of Solutions for Riemann Problems*, Notes on Numerical Fluid Mechanics, J. Ballman and R. Jeltsch, 24 (1989), 169–178.

[3] J. Glimm and D. Sharp, *An S-matrix Theory for Classical Nonlinear Physics*, Found. Phys., 16 (1986), 125–141.

[4] E. Isaacson, D. Marchesin and B. Plohr, *Transitional Waves for Conservation Laws*, SIAM J. Math. Anal., 21 (1990), 837–866.

[5] T. -P. Liu, *Nonlinear Stability of Shock Waves for Viscous Conservation Laws*, Mem. Amer. Math. Soc., 56 (1985), 1–108.

[6] ———, *Shock Waves for Compressible Navier-Stokes Equations are Stable*, Comm. Pure Appl. Math., 39 (1986), 565–594.

[7] T. -P. Liu and K. Zumbrun, *Nonlinear Stability of an Undercompressive Shock*, in preparation, (1992).

[8] D. Schaeffer and M. Shearer, *The Classification of* 2×2 *Systems of Non-Strictly Hyperbolic Conservation Laws, with Application to Oil Recovery*, Comm. Pure Appl. Math., 40 (1987), 141–178.

K. Zumbrun
Department of Applied Mathematics and Statistics,
State University of New York,
Stony Brook, NY 11794-3651
Current address:
Department of Mathematics,
Indiana University
Bloomington, IN 47405, USA

B. Plohr
Departments of Mathematics and of Applied Mathematics and Statistics,
State University of New York,
Stony Brook, NY 11794-3651

D. Marchesin
Instituto de Matematica Pura e Aplicada
22460 Rio de Janeiro RJ Brazil